Electronic Supplementary Material (ESI) for Nanoscale Horizons.
This journal is © The Royal Society of Chemistry 2019

Supporting Information

Surface Functionalized 3D Carbon Fibers Boosts the Lithium Storage Behaviour of Transition Metal Oxide Nanowires via Strong Electronic Interaction and Tunable Adsorption Energy

Lei Hu,[b†] Yingxia Gao,[a†] Tuzhi Xiong,[a] David Adekoya,[c] Weitao Qiu,[b] Hao Yang,[b] M.-Sadeeq (Jie Tang) Balogun,*[a] Shanqing Zhang,[c] Anlian Pan,[a] Yuping Li,*[a] and Yexiang Tong*[b]

[a]College of Materials Science and Engineering, Hunan University, Changsha 410082, Hunan, People's Republic of China.

[b]MOE of the Key Laboratory of Bioinorganic and Synthetic Chemistry, The Key Lab of Low-carbon Chemistry & Energy Conservation of Guangdong Province, KLGHEI of Environment and Energy Chemistry, School of Chemistry, Sun Yat-sen University, 135 Xingang West Road, Guangzhou 510275, People's Republic of China

[c]Centre for Clean Environment and Energy, Gold Coast Campus, Griffith University, Australia.

*E-mail: balogun@hnu.edu.cn

*E-mail: liypli@hnu.edu.cn

*E-mail: chedhx@mail.sysu.edu.cn

2. Experimental Section

2.1. Materials

Carbon cloth was purchased from Fuel Cell Earth LLC, United States. $Ni(NO_3)_2 \cdot 6H_2O$, hexamethylenetetramine, concentrated HNO_3, NH_4VO_3 and ethanol (99.7%) were all purchased from Guangzhou Chemical Reagent Factory and used as received without further purification.

2.2. Synthesis of PNCFC current collector

Firstly, PNCFC was prepared according to our previous report. [1] In a typical synthesis, after the cleaning of carbon fiber cloth (CFC) in concentrated HNO_3, distilled water and ethanol for several times, the clean CFC was immersed in a 30 min well–stirred solution of 10 mmol $Ni(NO_3)_2 \cdot 6H_2O$ and 20 mmol hexamethylenetetramine (HMT) dissolved in 40 mL of deionized water and vigorously stirred for another 10 min. The solution and CFC were transferred to a 50 mL Teflon-lined stainless-steel autoclave and heated in an electric oven with a heating speed of 10 ^oC min^{-1} to 120 ^oC and maintained in an oven for 10 h and then allowed naturally to cool to room temperature. After cooling down to room temperature, the Ni precursor/CFC was washed with water, ethanol for several times and dried in 60 ^oC oven overnight and annealed in the N_2 atmosphere at 900 ^oC for 90 min with a heating speed of 10 ^oC min^{-1} to 900 °C (200 sccm). The product obtained after annealing was then immersed in concentrated HCl for 12 h to remove the Ni NPs and obtain porous exfoliated N-doped CFC current collector (denoted as PNCFC).

2.3. Synthesis of PNCFC@V_2O_5

VO_x interwoven nanowires were first synthesized by a hydrothermal method reported elsewhere. [2] In a typical synthesis, 0.324 g of NH_4VO_3 was dissolved in a 40

mL solution mixture of water and ethanol (volume ratio: 9/1). The pH of the solution was adjusted to ~2 by HCl. As-prepared PNCFC was then immersed in a 50 mL Teflon-lined autoclave containing the NH_4VO_3 solution and heated up to 160 °C for 12 h, then allowed to cool to room temperature. The PNCFC@VO_x obtained was annealing in the air (ramping rate of 5 °C min^{-1}) at 400 °C for 3 h to achieve the PNCFC@V_2O_5.

2.4. Synthesis of CFC@V_2O_5

CFC@V_2O_5 was prepared exactly the same way as the PNCFC@V_2O_5 but untreated carbon fiber cloth (CFC) was used as the substrate instead of the PNCFC.

2.5. Characterization

Field emission SEM (JSM-6330F) and transmission electron microscope (TEM) (JEM2010-HR, 200 KV) were used to characterize the morphology, structure, and composition of the samples. X-ray Photoelectron Spectroscopy (XPS, ESCALab250) was used for element identification and heteroatom functional group distribution. X-ray diffraction Spectrometry (XRD; Shimadzu X-ray diffractometer 6000, Cu Kαradiation, Shimadzu, Tokyo, Japan) and Raman Spectroscopy (Renishaw inVia) were used to characterize the crystallographic information and phase purity of the samples.

2.6. Electrochemical Measurements

The Li storage performance tests were carried out via CR2032 coin type cells. The electrodes were first cut into many smaller square pieces with area of 1.0 cm^2. The cells were assembled in an argon-filled glove box [Mikrouna (China) Co., Ltd.] with the as-prepared samples as working electrode, Li foil as which serve as counter and reference electrode, Celgard 2400 separator as separator and 1 M $LiPF_6$ in 1:1 by volume of ethylene carbonate (EC)/dimethyl carbonate (DMC) as electrolyte.

Galvanostatic measurements were carried out on a Neware battery tester (CT-3008-164, Shenzhen, China) at a voltage range of 2.0-4.0 V (vs. Li/Li^+). Cyclic voltammetry (CV) and Electrochemical impedance spectroscopy (EIS) were conducted on the electrochemical working station (CHI 760E, Chenhua, Shanghai).

2.7. DFT Calculations

The entire calculations have been performed with the Vienna ab initio Simulation Package (VASP). [3] 3D periodic boundary conditions were used to simulate the infinitely large systems. The vacuum space between sheets was adjusted to 20 Å to prevent the two membrane layers interaction. The fibre Brillouin zone was sampled by 1 × 3 × 1 k-points. The system electronic structure was manipulated using the generalized gradient approximation with the PBE functional. [4] The van der Waals interactions were added to the standard DFT description by Grimme's D2 scheme. [5] All calculations include spin polarization. During the entire calculations, the convergence parameters were 10^{-6} eV for the energy, 0.01 eV $Å^{-1}$ for the forces and an energy cut-off of 500 eV. A Gaussian smearing of 0.05 eV was also applied. Charge analysis was performed via Bader analysis, [6] which included the core charges, and charge density difference analysis within VASP.

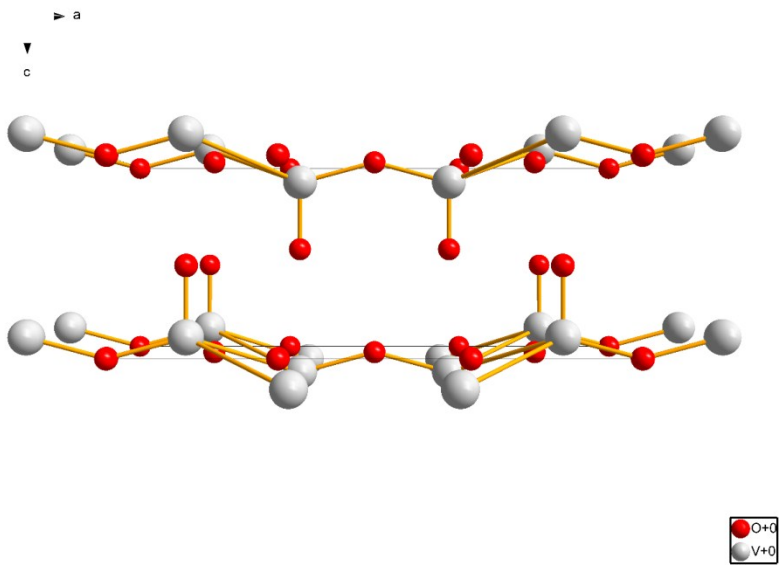

Figure S1. Optimized cluster structure of V_2O_5.

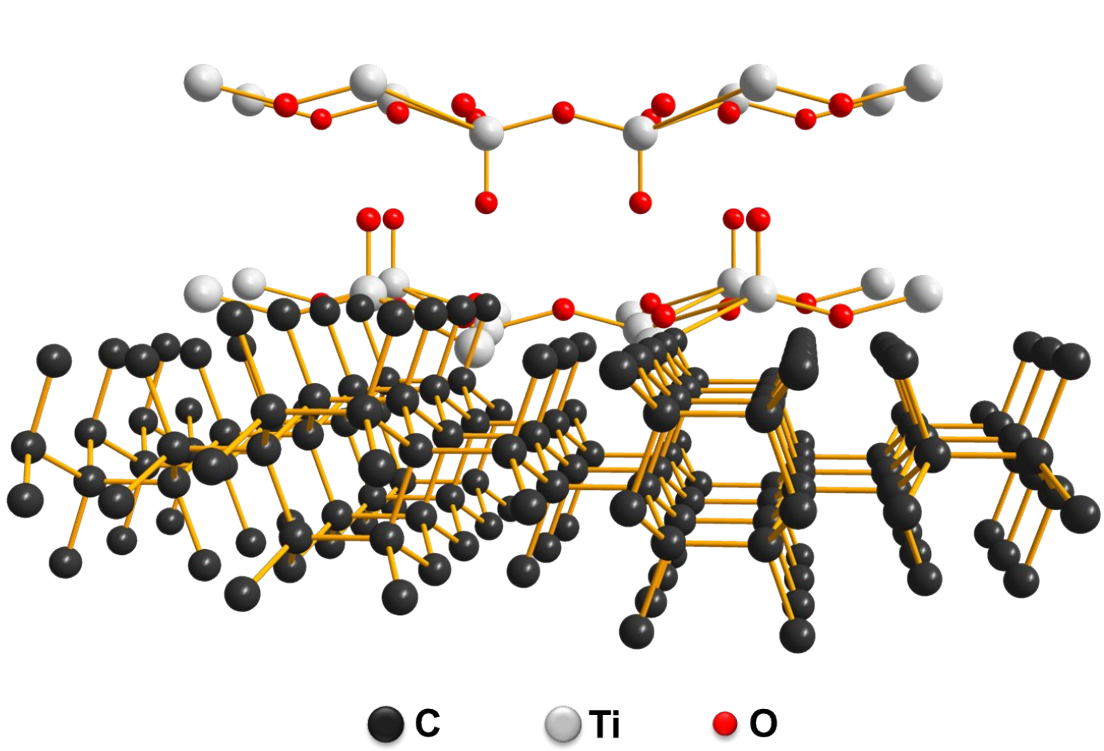

Figure S2. Optimized cluster structure of CFC@V_2O_5.

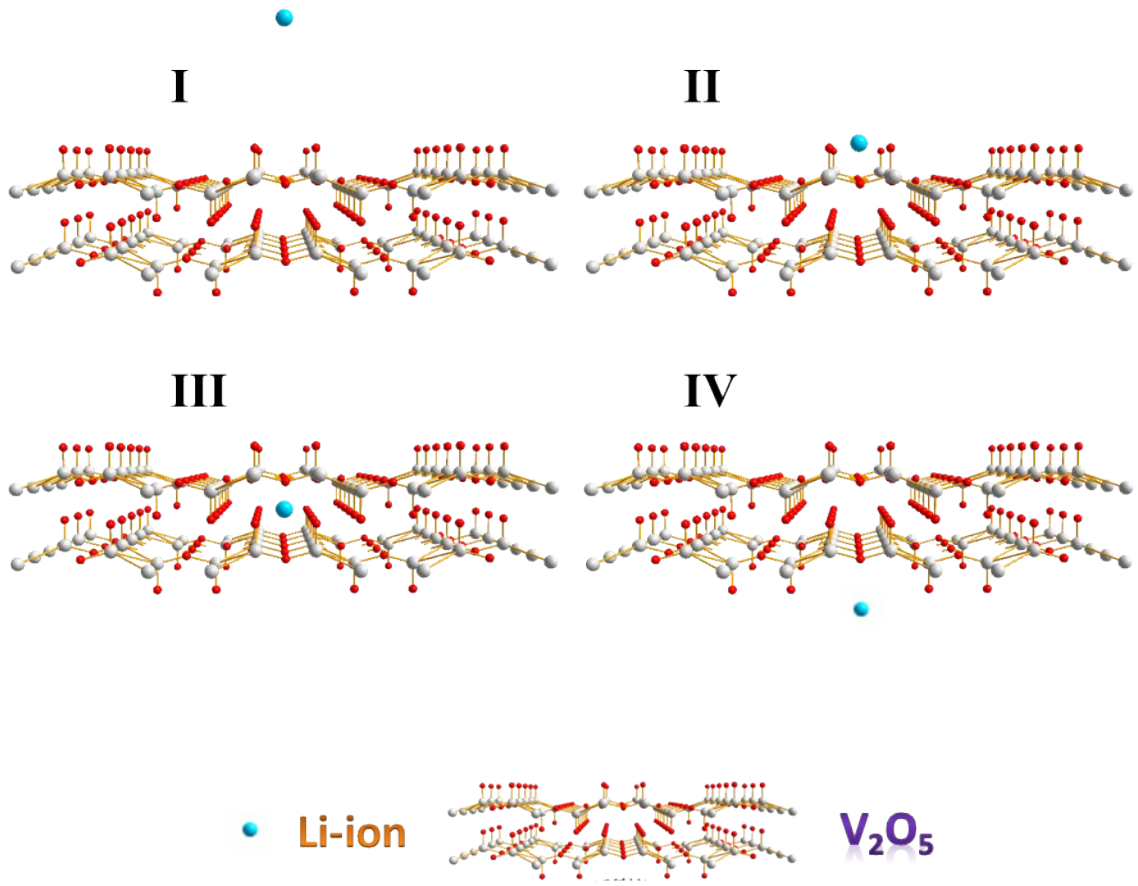

Figure S3. Optimized cluster structure of V_2O_5 with Li-ion intercalation site from point I-IV.

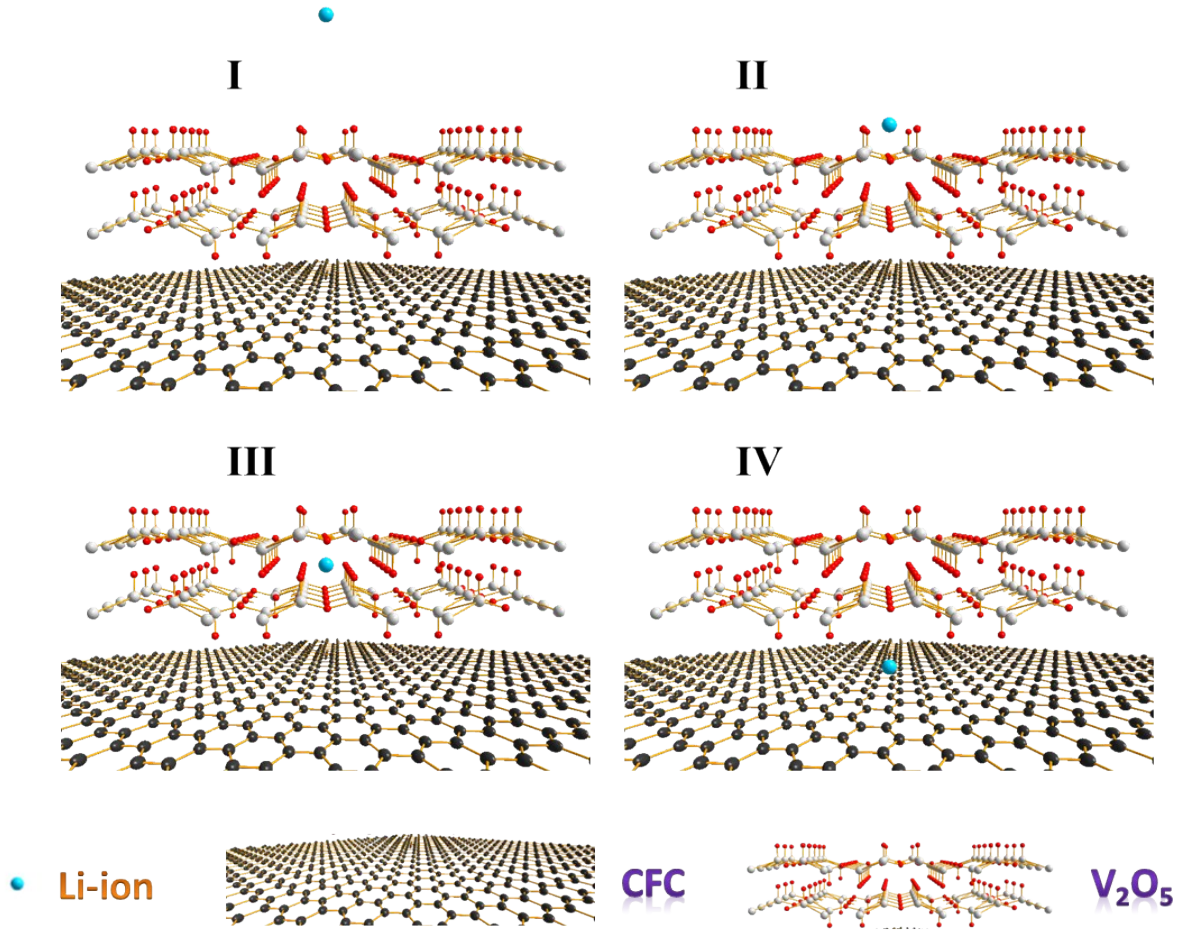

Figure S4. Optimized cluster structure of CFC@V_2O_5 with Li-ion intercalation site from point I-IV.

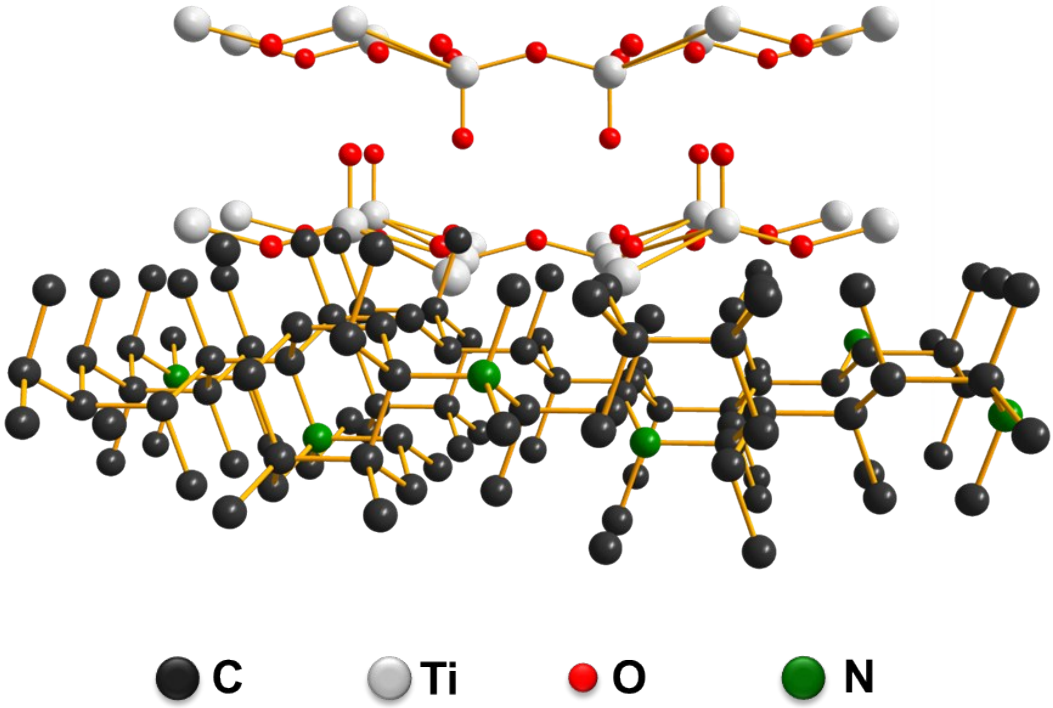

Figure S5. Optimized cluster structure of PNCFC@V_2O_5.

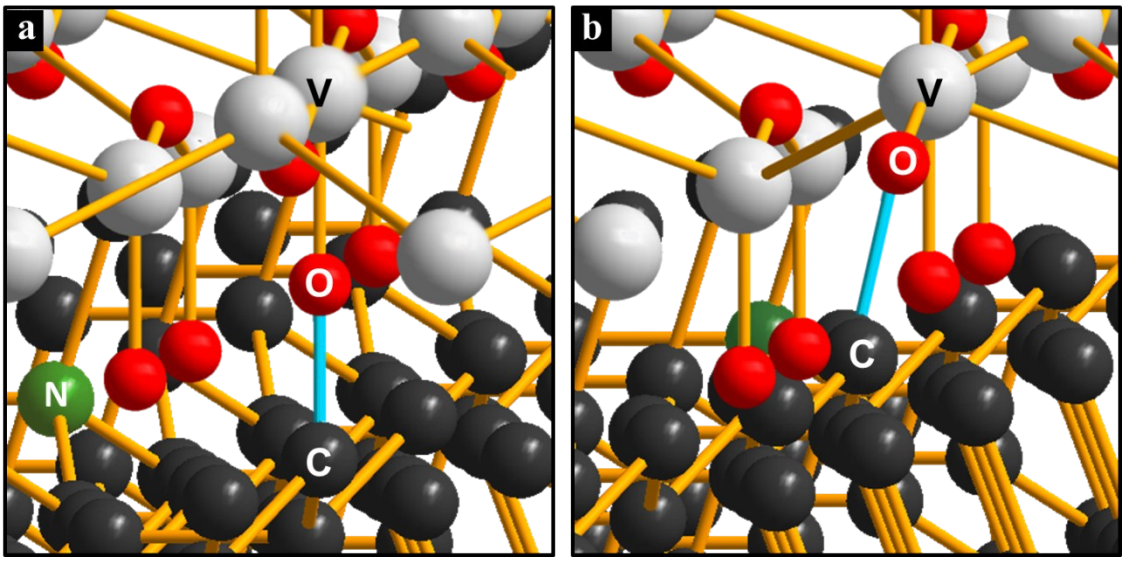

Figure S6. (a) Enlarged snapshot of covalent bonds between C (functional group of ECC) and O (from V_2O_5). (b) Enlarged snapshot of covalent bonds between O (functional group of ECC) and V (from V_2O_5).

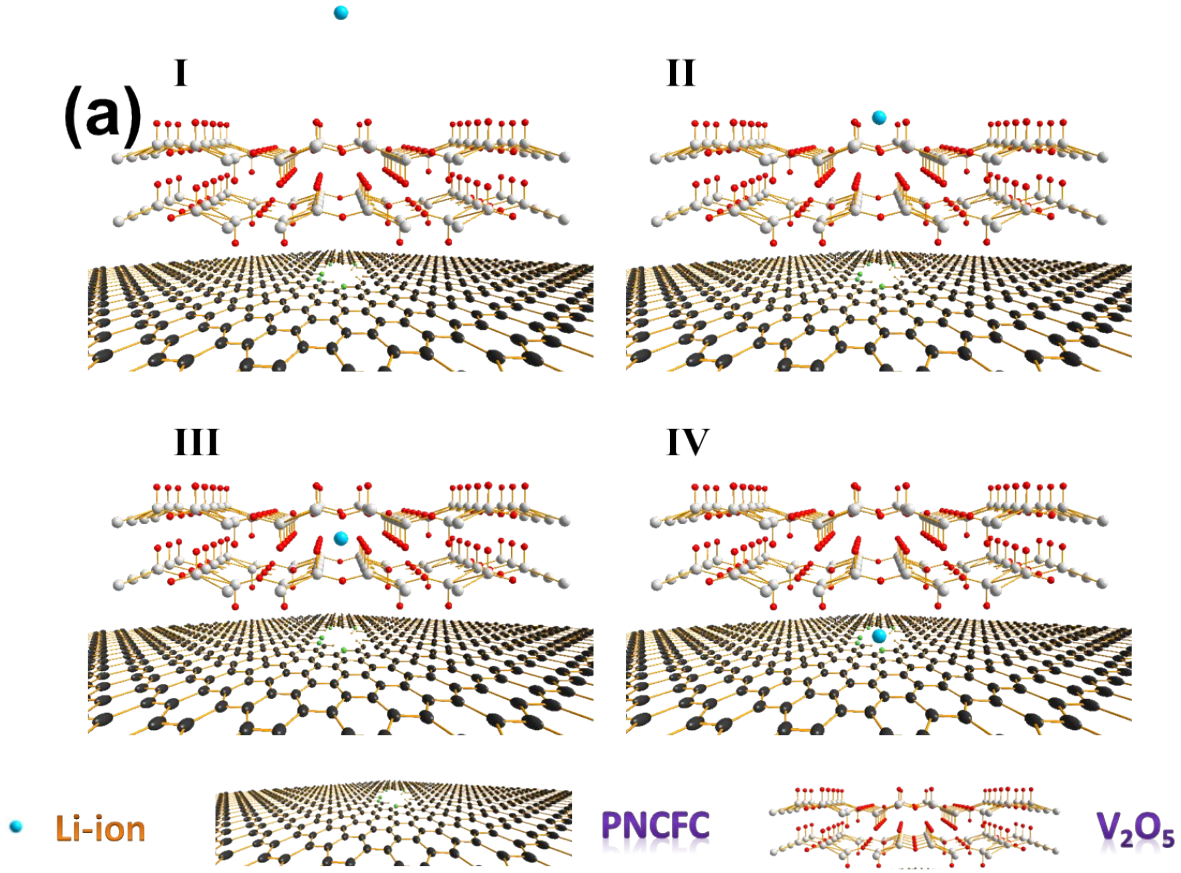

Figure S7. Optimized cluster structure of PNCFC@V_2O_5 with Li-ion intercalation site from point I-IV.

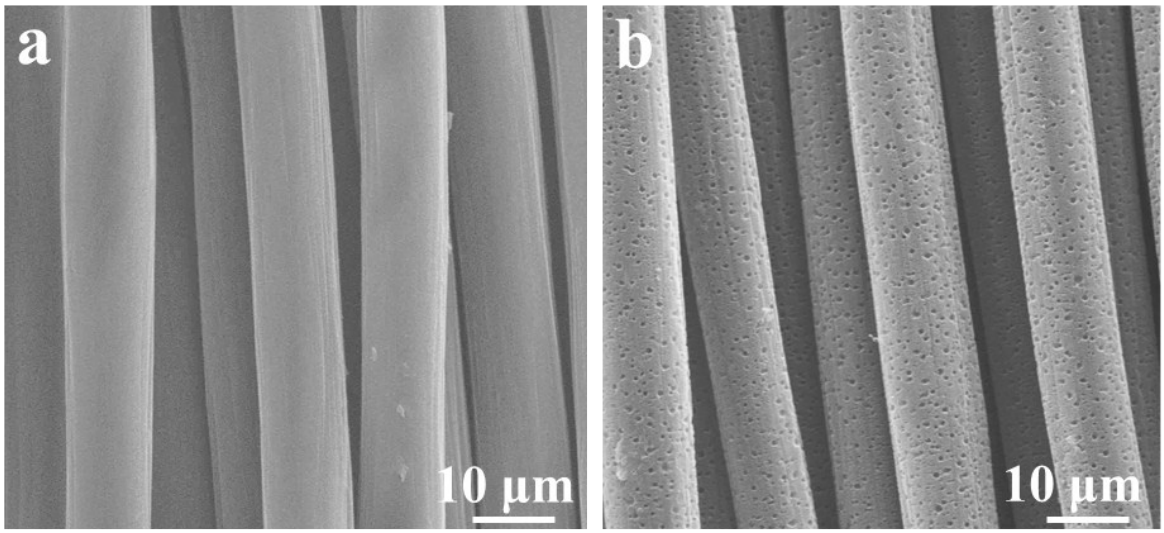

Figure S8. SEM images of (a) CFC and (b) PNCFC.

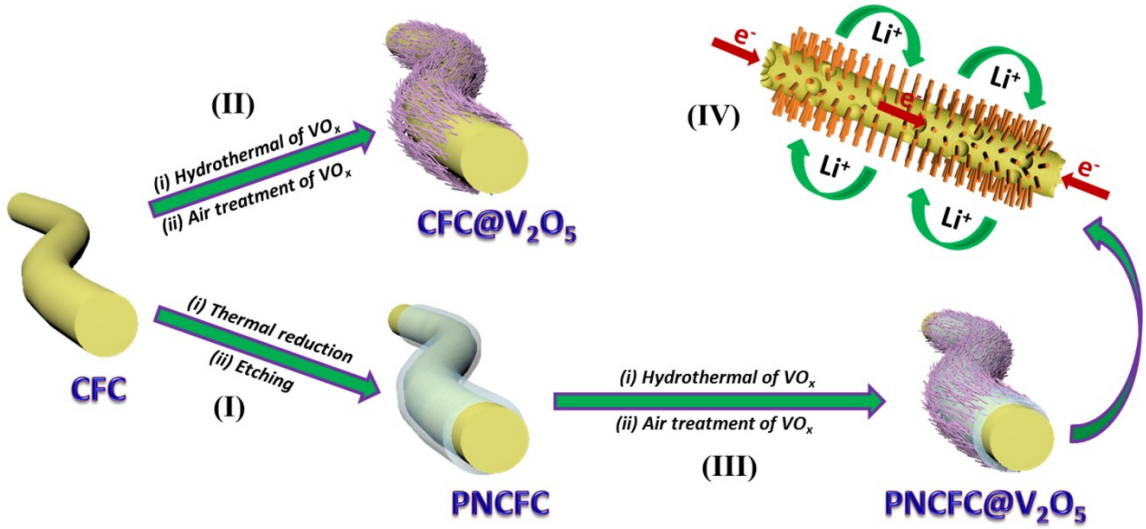

Scheme S1. Schematic illustrations of PNCFC@V_2O_5 NWs fabrication process. (I) PNCFC synthesis via hydrothermal and thermal etching. Hydrothermal growth of V_2O_5 NWs on (II) CFC and (III) PNCFC. (IV) Li ion and electron transfer routes of the PNCFC@V_2O_5 NWs.

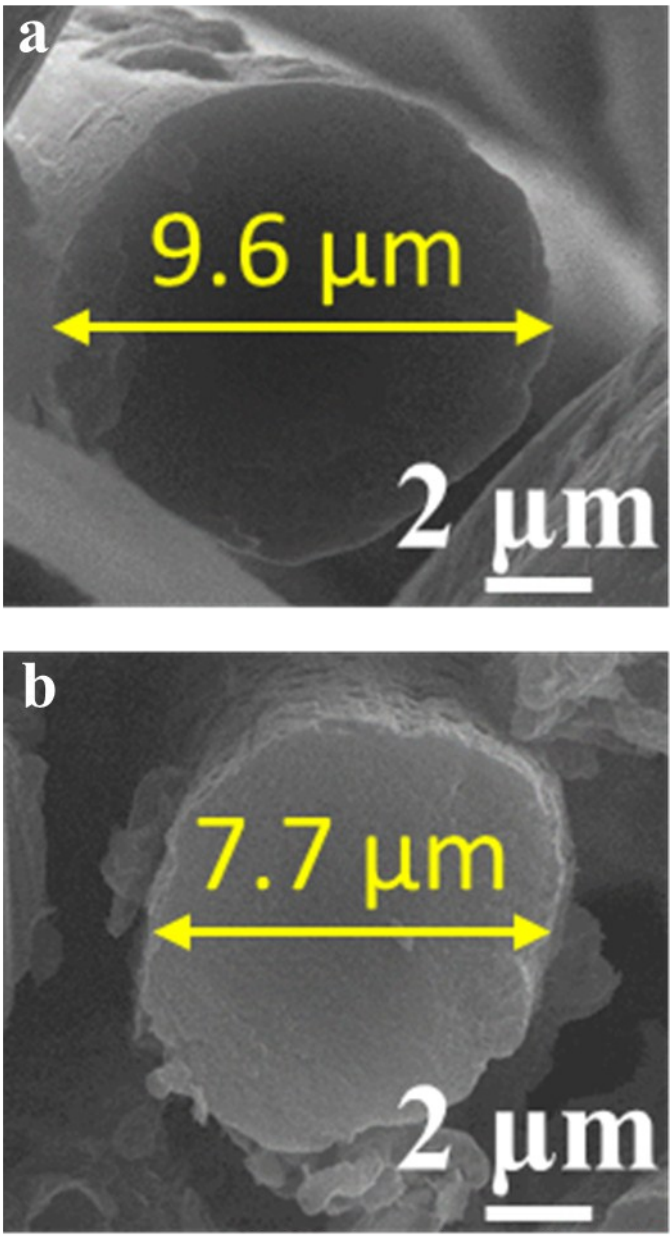

Figure S9.Cross-sectional SEM images showing the thickness of a single fiber for (a) CFC and (b) PNCFC current collectors.

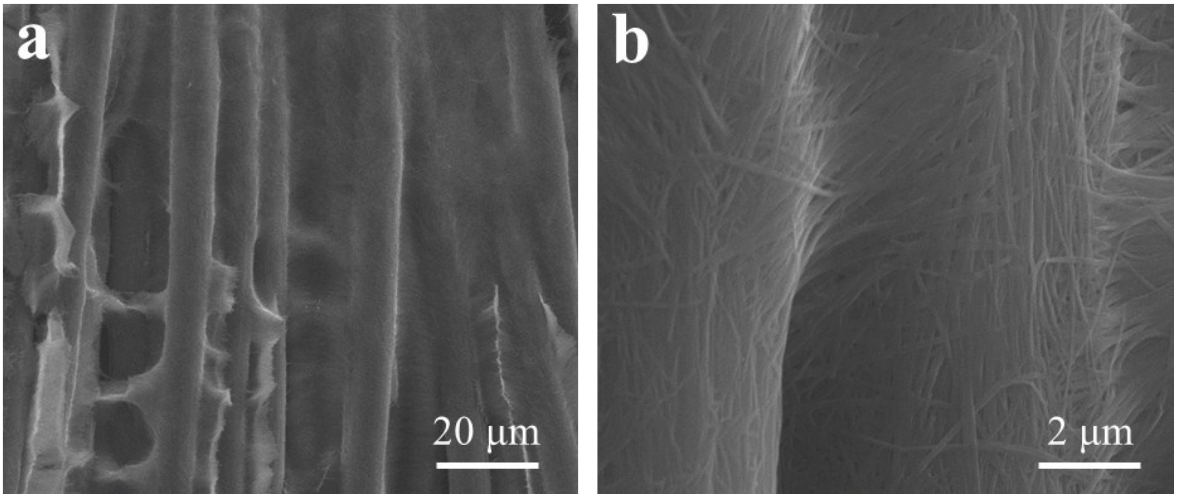

Figure S10. SEM images of the PNCFC@VO_x NWs.

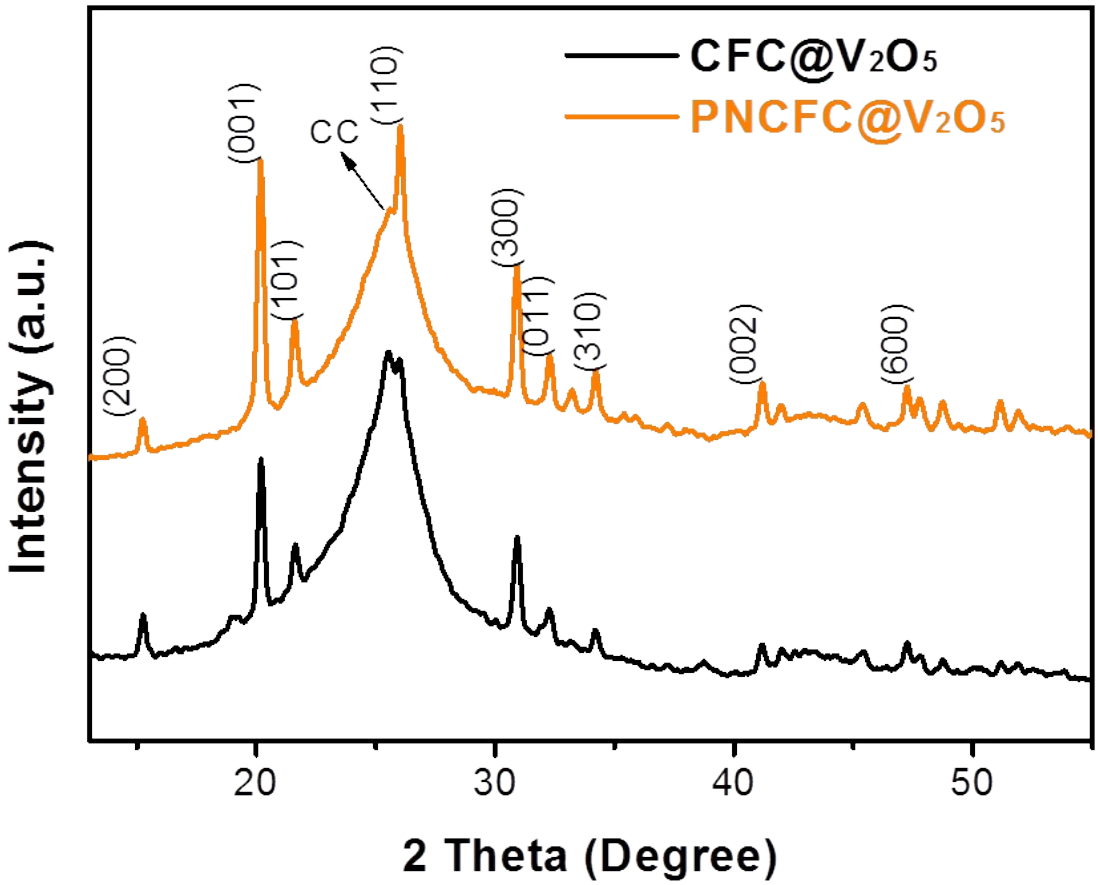

Figure S11. XRD patterns of the CFC@V_2O_5 and PNCFC@V_2O_5 NWs.

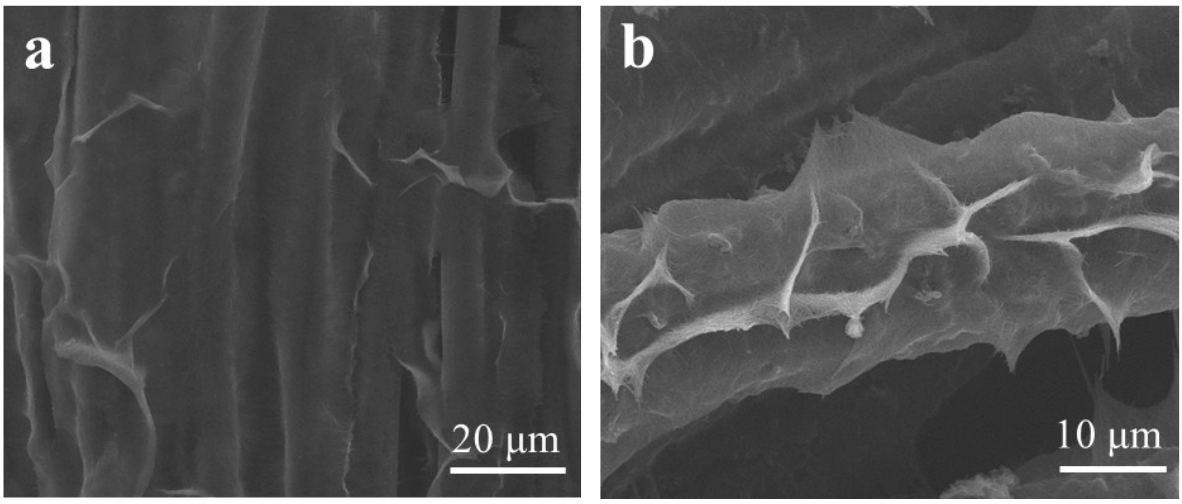

Figure S12. SEM images of CFC@V_2O_5 NWs.

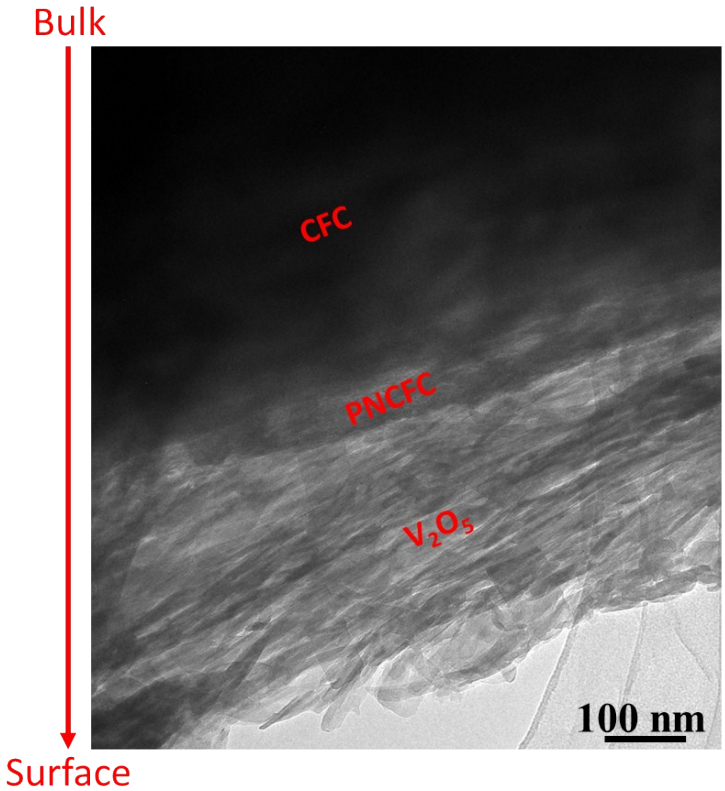

Figure S13. Enlarged image of PNCFC@V_2O_5 from Figure 1H.

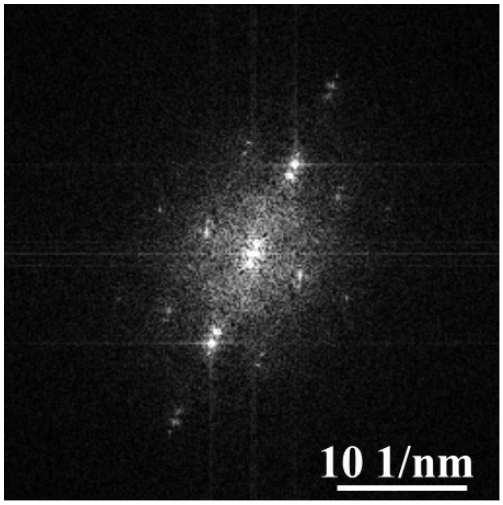

Figure S14. SAED pattern of PNCFC@V_2O_5.

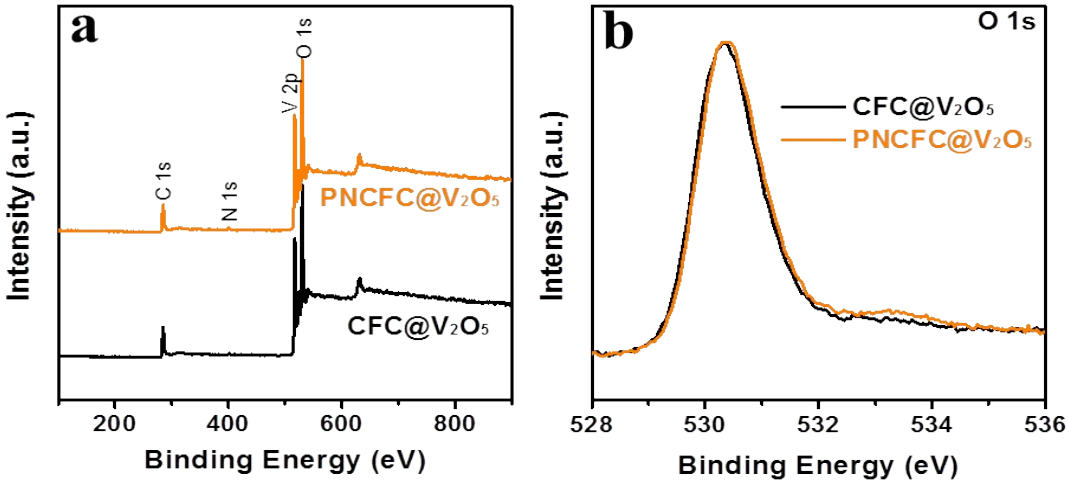

Figure S15. (a) XPS survey spectra and (b) O 1s XPS spectra CFC@V_2O_5 and PNCFC@V_2O_5.

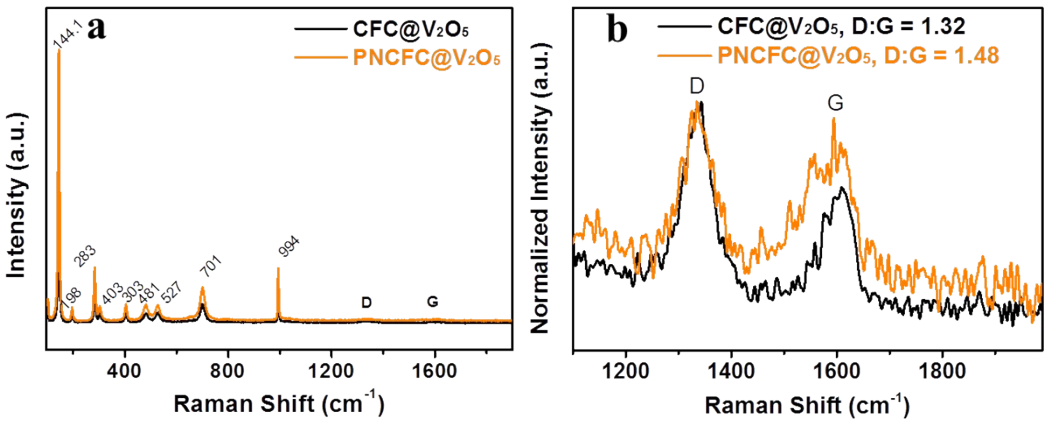

Figure S16. (a) Full Raman spectra and (b) Normalized intensity Raman spectra between 1100 and 1950 cm^{-1} of the CFC@V_2O_5 and PNCFC@V_2O_5 samples.

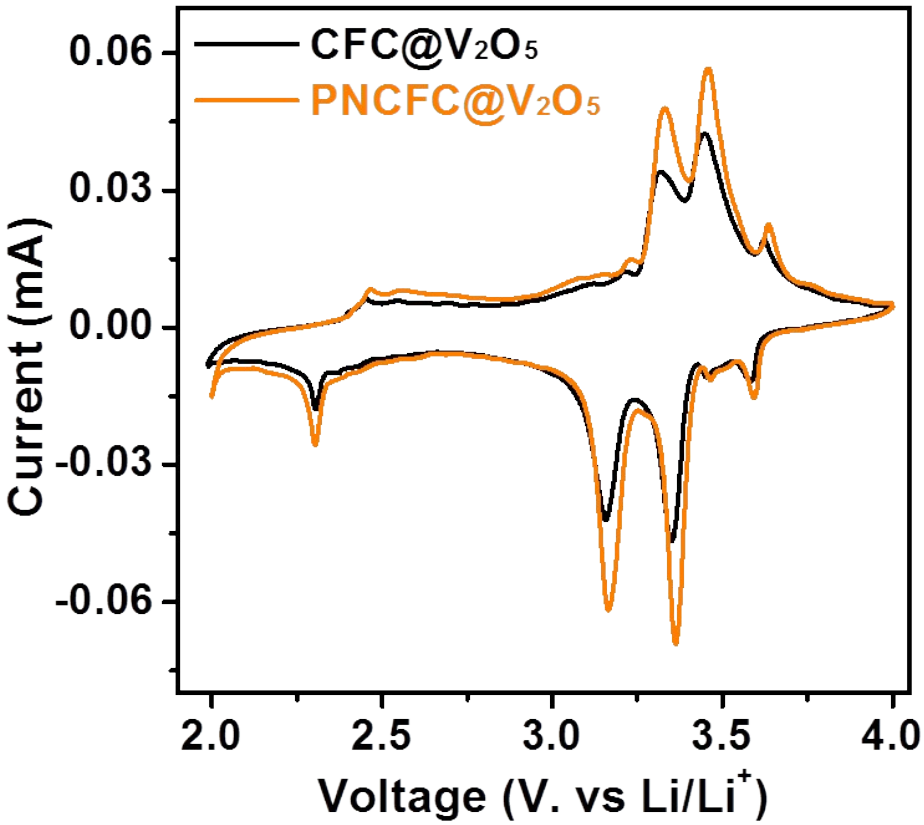

Figure S17. (a) CV curves of CFC@V_2O_5 and PNCFC@V_2O_5 electrodes.

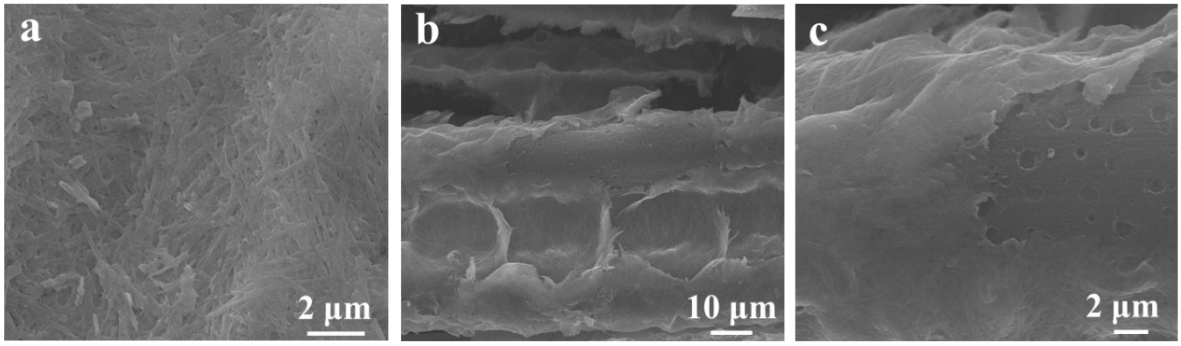

Figure S18. SEM images of PNCFC@V_2O_5 after electrochemical cycles.

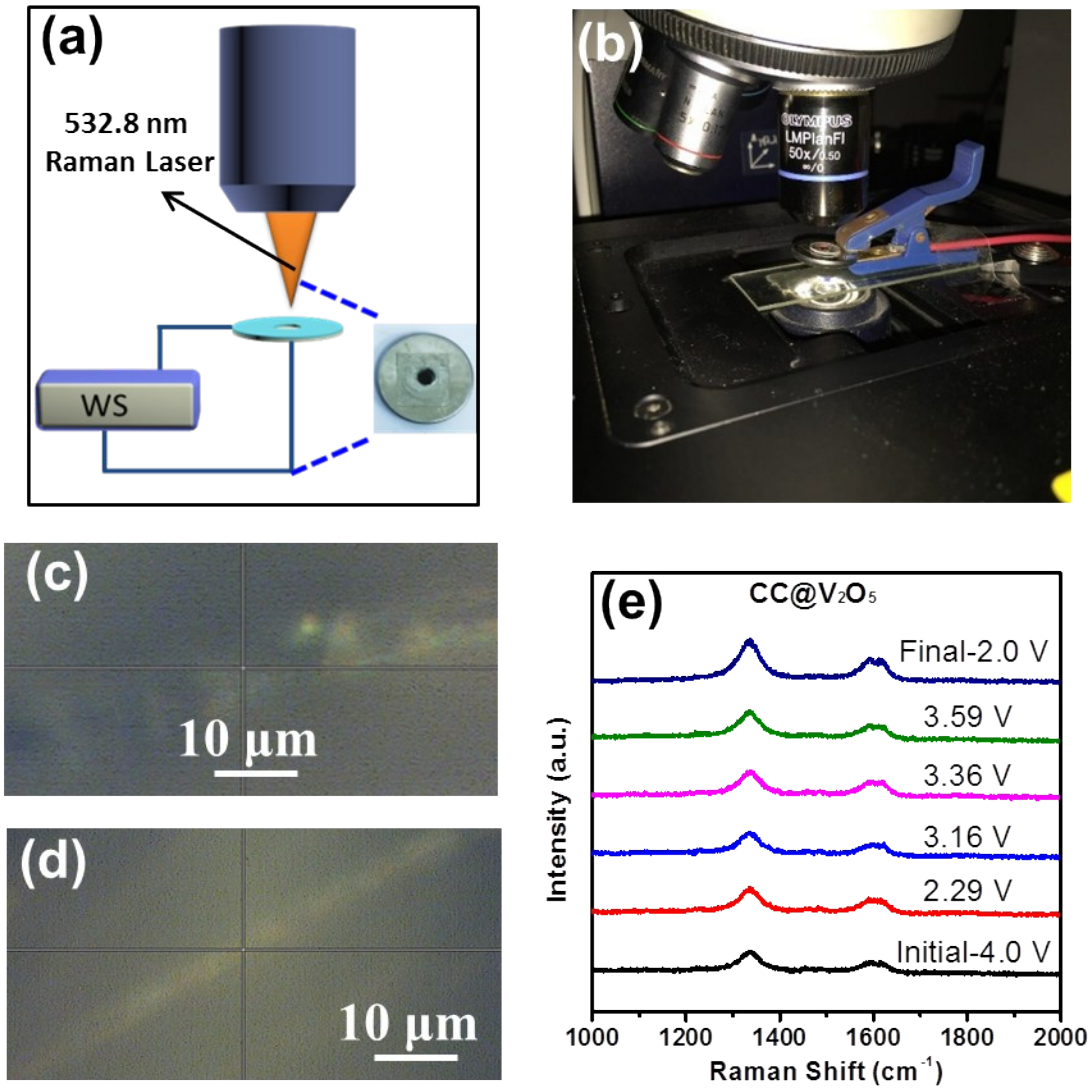

Figure S19. *In-situ* Raman analyses of the electrodes. (a) Schematic representation of the *in-situ* Raman analysis of the cells. (b) Digital image of the *in-situ* Raman analysis set-up. SEM image of the point where Raman spectra were collected for (c) CFC@V_2O_5 and (d) PNCFC@V_2O_5. (e) *In-situ* Raman spectra of PNCFC@V_2O_5 at different intercalated voltages. A schematic representation of the *in-situ* Raman set-up and digital image is presented in Figure S19a and S19b, respectively. Both electrodes were initially subjected to three electrochemical cycles and charged to 4.0 V before the *in-situ* experiment. The SEM images for both electrodes were also shown in Figures S19c-S19d.

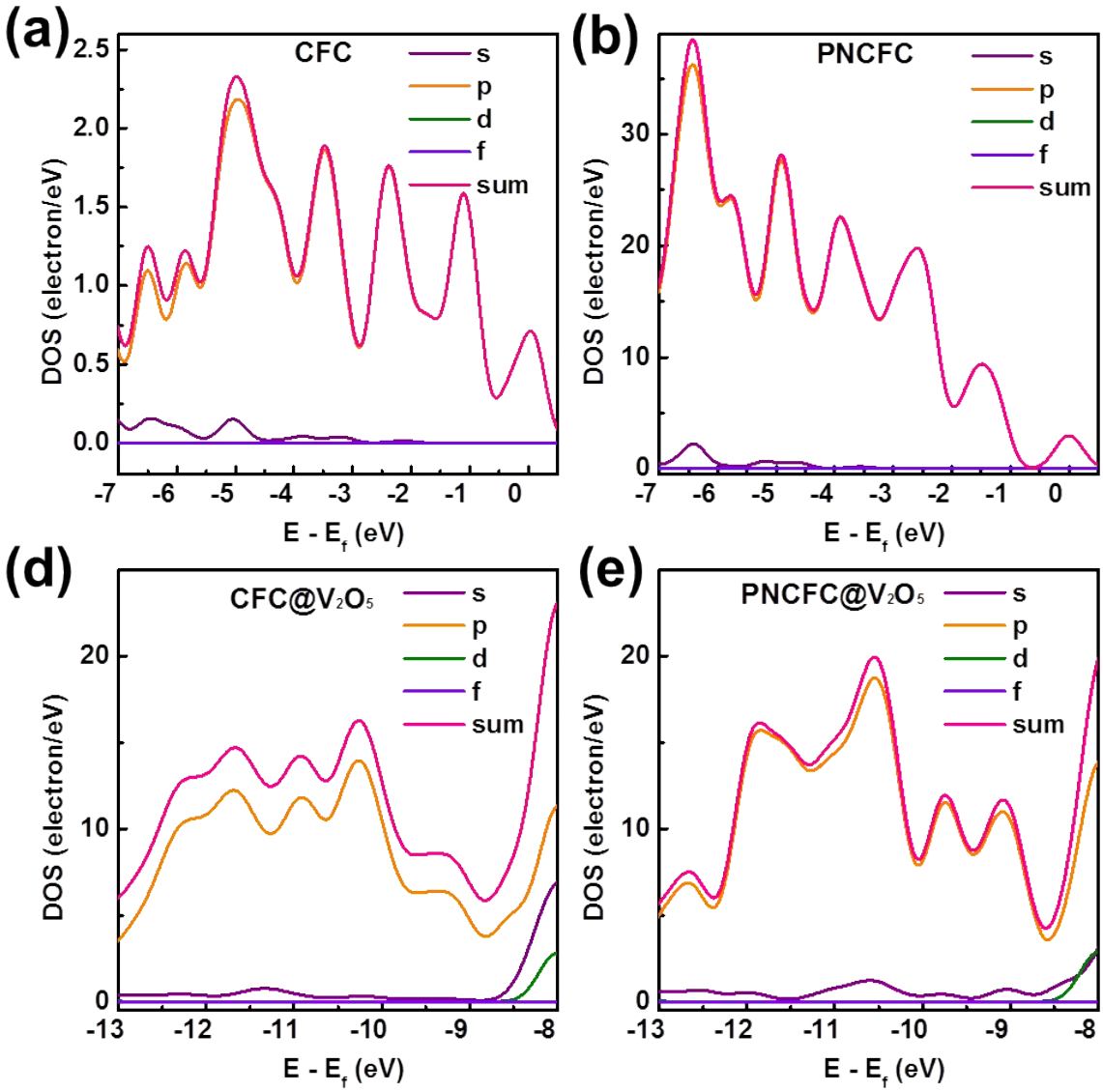

Figure S20. Calculated density of states (DOS) of (a) CFC, (b) PNCFC, (c) CFC@V_2O_5 and (d) PNCFC@V_2O_5 showing their corrrepsonding s-, p-, d-, f- and sum-adsoprtion energy levels.

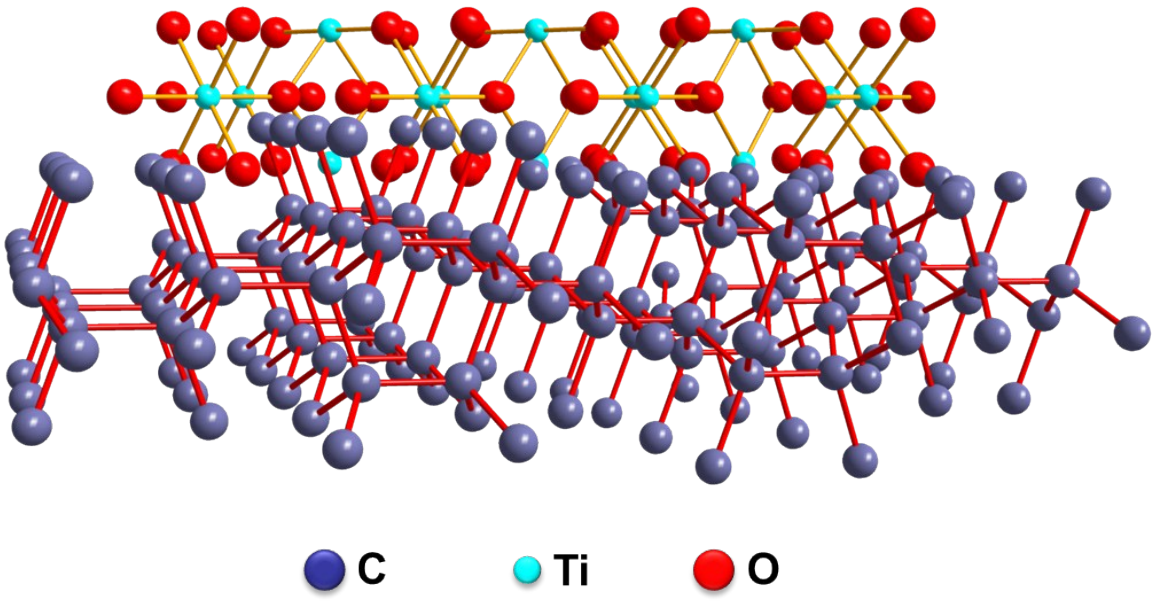

Figure S21. Optimized clusters structure for CFC@TiO_2.

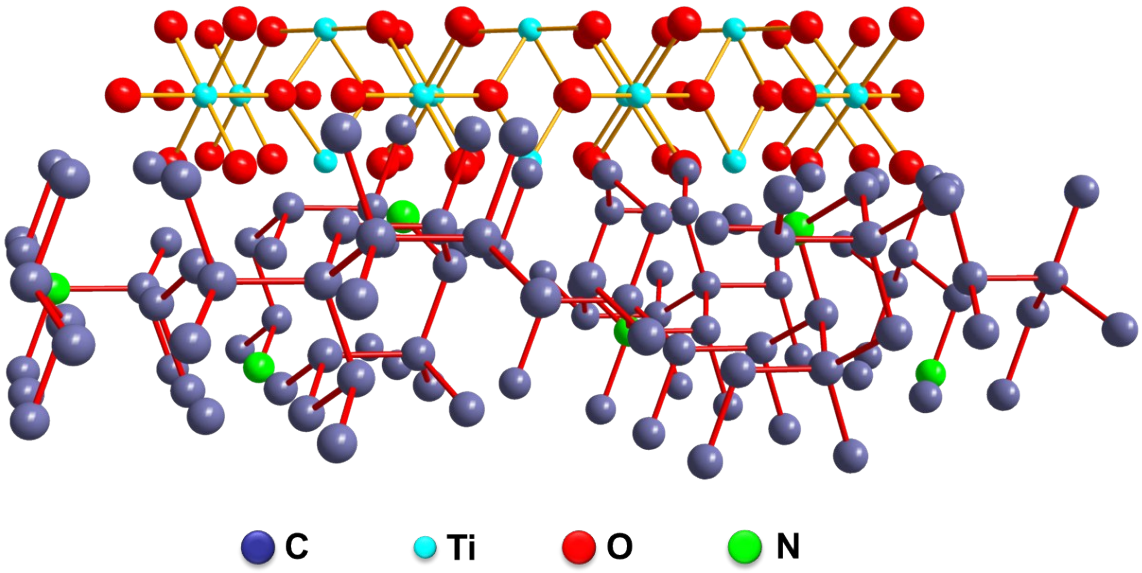

Figure S22. Optimized clusters structure for PNCFC@TiO_2.

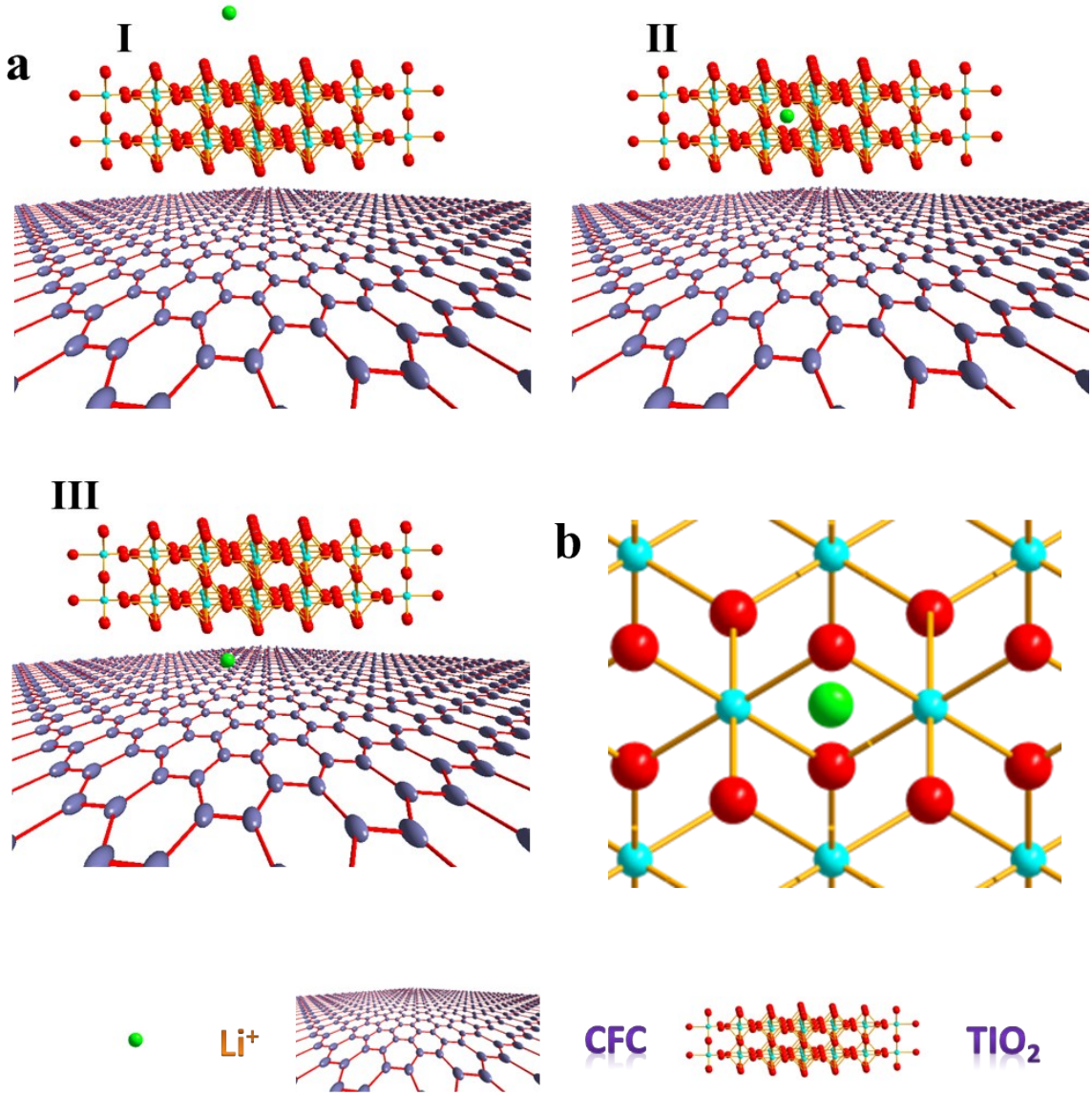

Figure S23. (a) Optimized cluster structure of CFC@TiO_2 with Li-ion intercalated site. (b) Enlarged snapshot of Li-ion passing through TiO_2 of CFC@TiO_2.

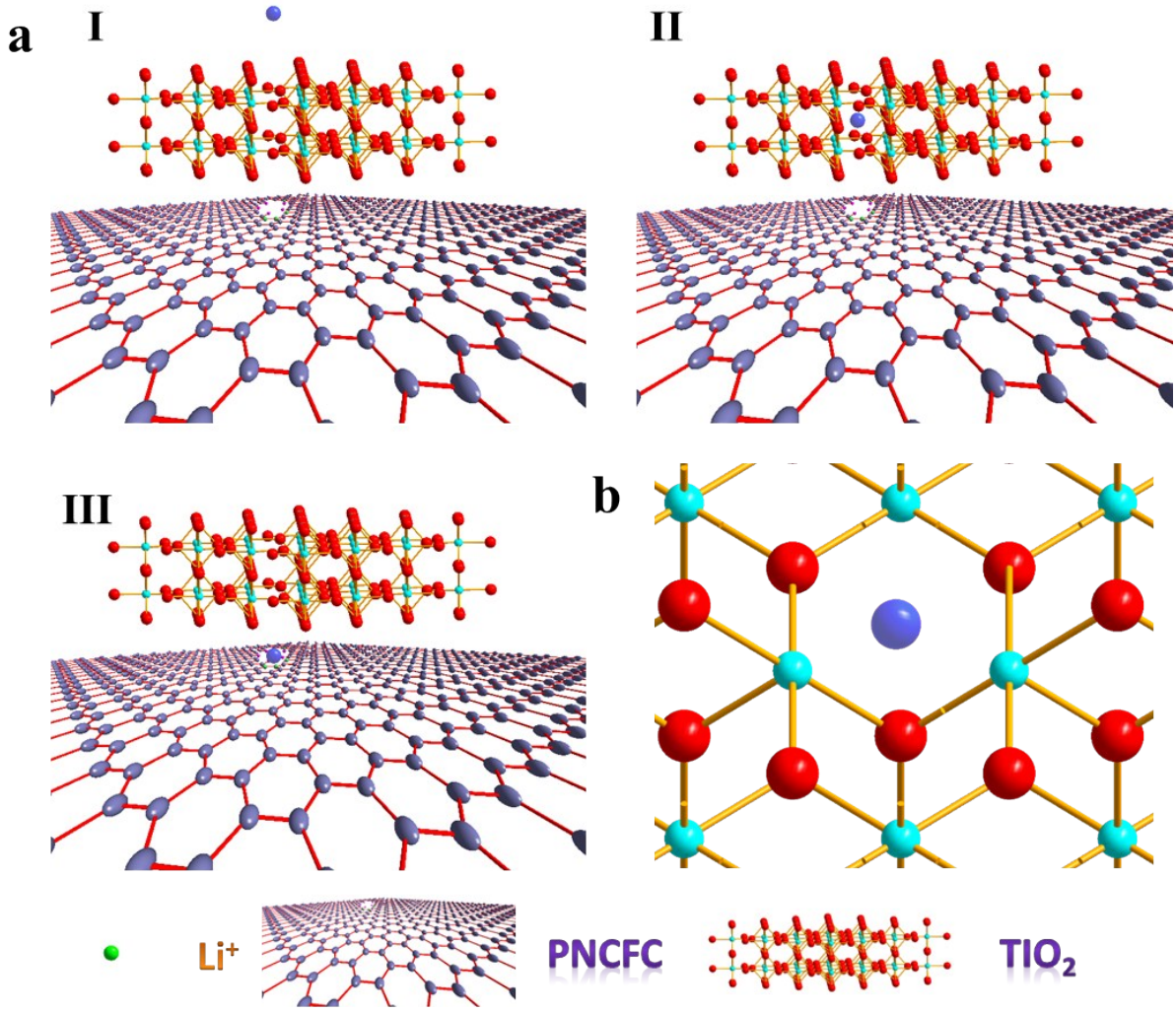

Figure S24. (a) Optimized cluster structure of PNCFC@TiO_2 with Li-ion intercalated site. (b) Enlarged snapshot of Li-ion passing through TiO_2 of PNCFC@TiO_2.

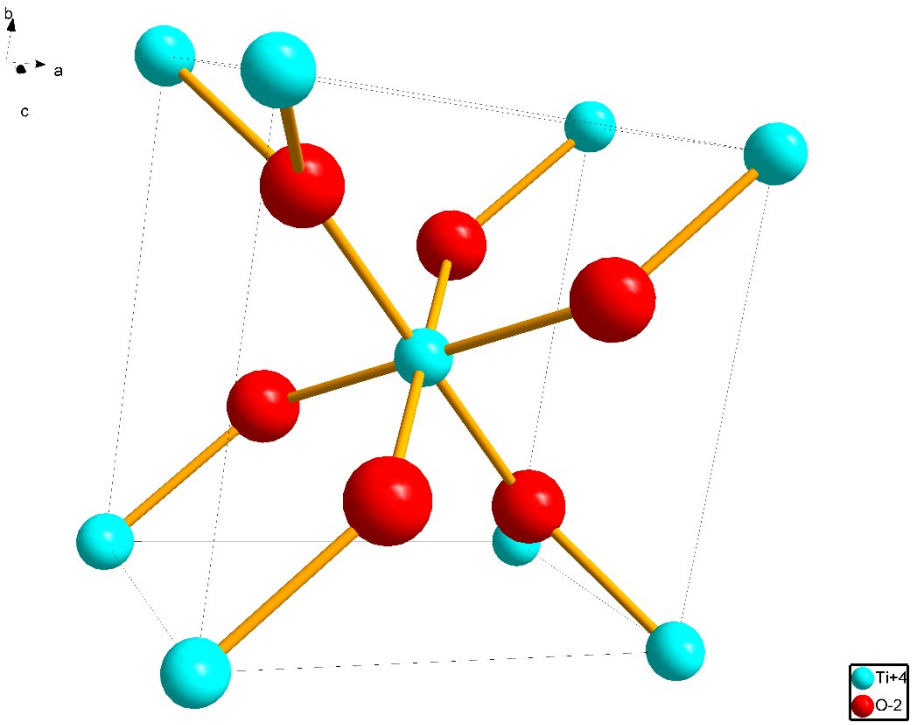

Figure S25. Optimized clusters structure for TiO_2.

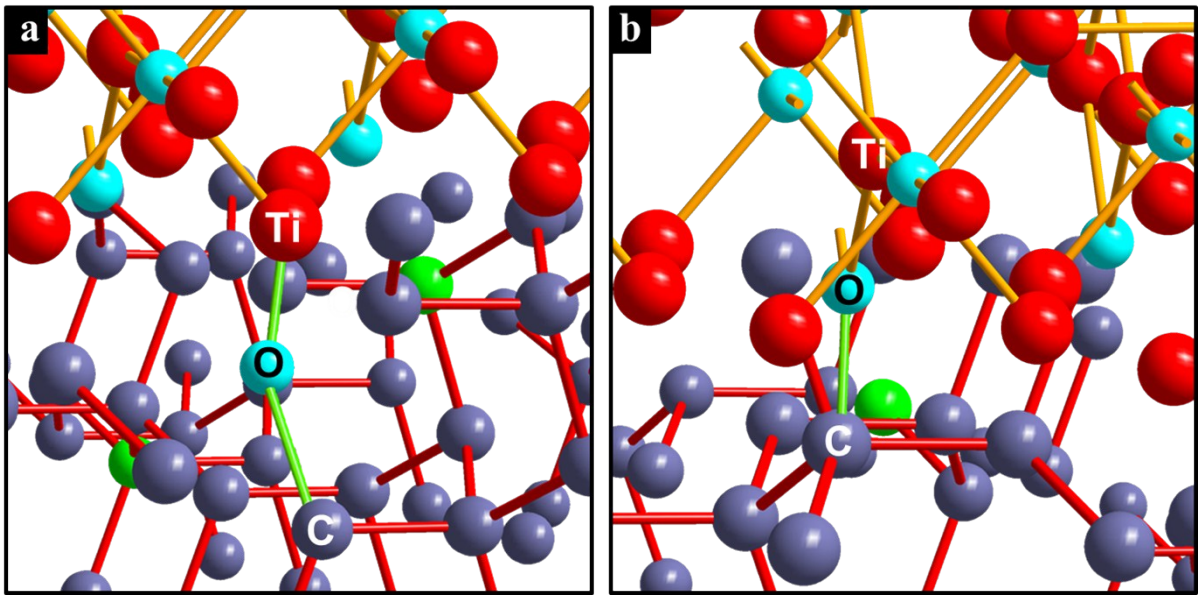

Figure S26. (a) Enlarged snapshot of covalent bonds between O (functional group of ECC) and Ti (from TiO_2) and (b) Enlarged snapshot of covalent bonds between C (functional group of ECC) and O (from TiO_2).

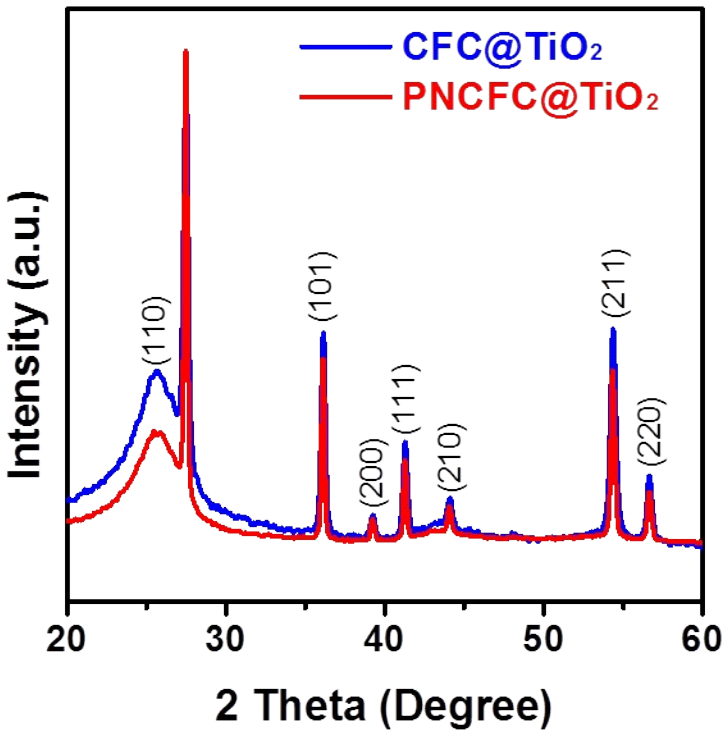

Figure S27. XRD patterns of the CFC@TiO_2 and PNCFC@TiO_2 NWs.

References

1. M.-S. Balogun, W. Qiu, H. Yang, W. Fan, Y. Huang, P. Fang, G. Li, H. Ji and Y. Tong, *Energy Environ. Sci.*, 2016, **9**, 3411-3416.
2. M.-S. Balogun, Y. Luo, F. Lyu, F. Wang, H. Yang, H. Li, C. Liang, M. Huang, Y. Huang and Y. Tong, *ACS Appl. Mater. Interfaces*, 2016, **8**, 9733-9744.
3. G. Kresse and J. Furthmüller, *Phys. Rev. B*, 1996, **54**, 11169-11186.
4. J. P. Perdew, K. Burke and M. Ernzerhof, *Phys. Rev. Lett.*, 1996, **77**, 3865-3868.
5. S. Grimme, *J. Comput. Chem.*, 2006, **27**, 1787-1799.
6. E. Sanville, S. D. Kenny, R. Smith and G. Henkelman, *J. Comput. Chem.*, 2007, **28**, 899-908.